

Gas-filled microspheres as an expandable sacrificial template for direct casting of complex-shaped macroporous ceramics

Linnéa Andersson, Lennart Bergström*

Materials Chemistry Research Group, Department of Physical, Inorganic and Structural Chemistry, Arrhenius Laboratory, Stockholm University, 10691 Stockholm, Sweden

Received 16 February 2008; received in revised form 14 April 2008; accepted 19 April 2008
Available online 9 June 2008

Abstract

Expandable microspheres have been used as a sacrificial template to produce macroporous ceramic materials by a gel-casting process. The temperature range for the gel-casting process has been tuned to allow the gas-filled polymer spheres to expand prior to the setting of the powder body. It is demonstrated that by controlling the amount and size of the expandable microspheres it is possible to tune and tailor the porosity up to 86% and the pore size distribution from 15 up to 150 μm . The expandable microspheres add a relatively low amount of organic material that allows rapid and facile burn-out. The temperature-induced expansion of the microspheres and the associated volume increase of the suspension has been used as a simple zero-pressure near-net shaping method to yield complex-shaped macroporous alumina bodies.

© 2008 Elsevier Ltd. All rights reserved.

Keywords: Gel-casting; Macroporosity; Al_2O_3 ; Near-net shape; Expandable microspheres

1. Introduction

Macroporous ceramics are finding increasing use in a wide range of industrial areas.^{1–3} Established applications such as molten metal filtration,^{4–6} catalyst supports,^{7–9} and thermal insulation materials in, e.g. kilns¹⁰ are complemented with tailored materials for tissue engineering and scaffolds for bone replacement.^{11–13} Each application has specific demands on the features and properties of the porous ceramic material, e.g. porosity, pore size distribution, pore morphology and the pore connectivity (commonly identified as the relation between open and closed porosity). The high permeability and high surface area that, e.g. characterise porous materials used in various catalysis applications require a high open porosity and hierarchical pore size distribution,^{7,8,14} while thermal insulation materials in kilns utilize the inherent high melting point and high specific strength of, e.g. alumina or cordierite in combination with the high thermal shock resistance of ceramic foams.¹⁰ For molten metal filtration it is important to produce refractory and corrosion resistant ceramic foams with a well defined and consistent

pore size and connected (open) porosity.^{4,15,16} The combination of a suitable ceramic material¹⁷ with a tailor-made porosity, pore size distribution and pore connectivity^{18–20} is even more critical in tissue engineering applications where the implanted material should mimic the structure and material properties of cancellous bone.^{21,22}

There has been a significant development of various processing methods for the preparation of macroporous ceramics during the last 10–15 years.^{3,23–25} It is possible to identify three different fabrication routes: the replica, the sacrificial template and the direct foaming methods.²³ In the replica technique, a foam, e.g. a polymer foam, is impregnated with a slurry.²⁵ While this simple and straightforward process already is established in industry to produce, e.g. porous materials for molten metal filtration and diesel engine exhaust filters,^{1,3,23,26} there are limitations with respect to the mechanical stability and pore size. The replica method results in hollow struts^{2,27} and it is difficult to produce materials with pore sizes smaller than 200 μm .²³ In the sacrificial template method, a negative replica is generated as the templating material, e.g. dense or hollow polymer beads,^{28–31} is removed. The size, shape and arrangement of the templating material offers significant versatility to independently tailor the porosity, pore size distribution and pore morphology. However, the removal of the organic templating material can be very

* Corresponding author. Tel.: +46 8 162368; fax: +46 8 152187.
E-mail address: lennartb@inorg.su.se (L. Bergström).

time consuming and may also induce stresses and thus cause cracking and deformation of the material.³² The direct foaming technique relies on the use of surfactants³³ or particles³⁴ to stabilize a foam generated by, e.g. mechanical frothing or bubbling of a gas through a suspension. This technique allows easy and fast production of highly porous ceramic materials.²³ Compared to the replication method, the porosity created by direct foaming is generally less open with dense struts which results in lower permeability and higher strength.^{2,3}

In this work we combine gel-casting with a novel sacrificial templating material: expandable polymeric microspheres. The commercially available microspheres have already found industrial use in polymer-based applications such as acoustic insulation and to reduce the weight in vehicles.³⁵ Recently, the expandable microspheres have also been used to control the flow in microfluidic systems.³⁶ We show that the microspheres can be distributed homogeneously in the suspension to create a porous structure upon expansion. It is also demonstrated how the temperature-induced expansion of the microspheres can be used to directly cast macroporous bodies of a complex shape.

2. Experimental procedure

2.1. Materials

The commercially available alumina powder, AKP-30 (Sumitomo Chemical Co., Ltd., Japan) with an average particle size (D_{50}) of 0.31 μm and a specific surface area of 6.8 m^2/g , was used as a raw material. An ammonium polyacrylate (Darvan 821A, Vanderbilt Company Inc., USA) was used as dispersant. Methacrylic acid (MA) (Sigma–Aldrich Sweden AB, Sweden) and *N,N'*-methylenebisacrylamide (MBAM) (Sigma–Aldrich Sweden AB, Sweden) was used as the monomer and cross-linker, respectively. The total amount of monomer and cross-linker with respect to water was 15 wt.% and the weight ratio of MA:MBAM was 6:1. Ammonium persulfate (APS) (Sigma–Aldrich Sweden AB, Sweden) was used as the initiator for the radical polymerisation of the monomer and cross-linker. The added APS corresponded to 4.75 wt.% with respect to the total amount of monomer and cross-linker. 1-Octanol (Sigma–Aldrich Sweden AB, Sweden) was used as an antifoaming agent.

The expandable microspheres is a commercial product (Expancel, Sweden) that consist of a co-polymer shell of e.g. acrylonitrile, methacrylate and acrylate and are filled with a blowing agent (isobutane). The expandable microspheres used in this study; 551DU40, 820DU40 and ON316WUX, have a mean particle size (D_{50}) of 10–16 μm (551DU40 and 820DU40) and 33 μm (ON316WUX), in the unexpanded state. The as-received microspheres 551DU40 and 820DU40 were delivered in dry form while the ON316WUX microspheres were delivered in a wet state with 30 wt.% water content.

2.2. Procedure

The flow chart in Fig. 1 gives an overview of the process. The preparation of the gel-casting suspensions was performed in several steps. In the first step, half of the alumina powder

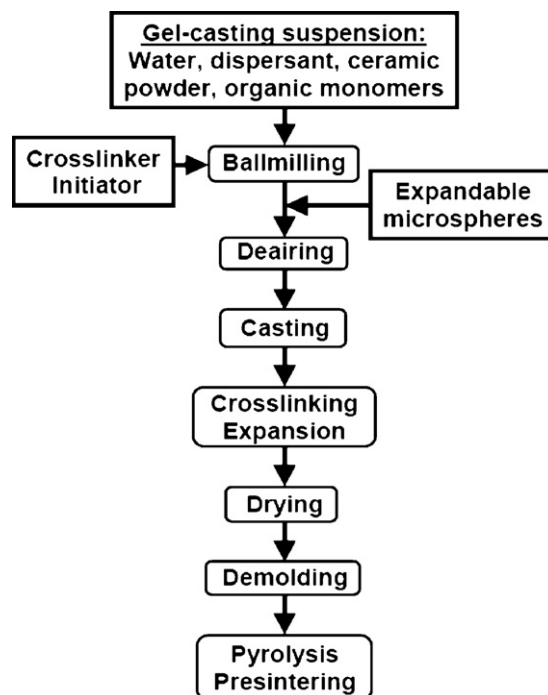


Fig. 1. Flow chart of the process. The microspheres are added after ball-milling to minimize mechanical-induced rupture.

was dispersed by stirring for 2 min in a solution containing the milling beads, the dispersant, the antifoaming agent and water. Then, a concentrated monomer/cross-linker premix solution with a monomer to water ratio of 3:1 was added during continuous stirring. In the final step, the remaining amount of alumina was added, the pH of the suspension was adjusted to 9.3 with ammonia (25 wt.%, aq.) and the suspension was homogenized by ball-milling in a planetary milling machine (PM 100, Retsch, Germany) for 25 min. The initiator (APS) was added at the end of the ball-milling process to avoid premature polymerisation of the suspension. The expandable microspheres were added and homogeneously distributed in the ceramic suspension by mechanical stirring after the ball-milling step was completed. The suspension was degassed for 6 min before the suspension was cast in high-density polyethylene moulds and simply placed in an oven preheated to 80 °C.

The gelled powder bodies were dried in a climate chamber (KBF 115, Binder, Germany) at an initial humidity of 70% relative humidity (RH) and temperature of 30 °C. The humidity was decreased stepwise to 30% (RH) and the temperature increased to 40 °C during a time period of 96 h.

The organic components were removed by burn-out in air at 600 °C for a period of 3 h. The macroporous alumina bodies were presintered at 1200 °C for 1 h (heating rate 5 °C min^{-1}).

2.3. Characterization

The scanning electron microscopy (SEM) was performed with a field emission gun scanning electron microscope (FEG-SEM), JSM-7000F (JEOL, Japan) at an acceleration voltage of 5 kV, and with a JSM-820 (JEOL, Japan) at an acceleration voltage of 7 kV.

The temperature of the suspensions was monitored with a thermocouple and logged every 5 s. The on-set temperature of the polymerisation was characterised by differential scanning calorimetry (DSC) (PerkinElmer Pyris 1, Wellesley MA) at a temperature increase rate of $5\text{ }^{\circ}\text{C min}^{-1}$. The DSC measurements were performed on suspensions dispensed in stainless steel capsules ($60\text{ }\mu\text{L}$) sealed with an O-ring to suppress the evaporation of water during heating (LVC, PerkinElmer). As a reference, an empty capsule was used. Thermal gravimetric analysis was performed in technical air at a heating rate of $10\text{ }^{\circ}\text{C min}^{-1}$ (PerkinElmer, Thermogravimetric Analyzer, TGA 7).

The porosity and density of the presintered bodies were evaluated using water as immersion liquid. The porous body was dried to a constant weight at $120\text{ }^{\circ}\text{C}$ and then cooled to room temperature in a desiccator. The dry porous body was weighed in air and then evacuated and infiltrated with distilled water which fills the open pores. The water-filled porous ceramic was weighed in air and the volume and open porosity of the porous body was calculated. The porous materials were also evaluated by mercury intrusion porosimetry (Micromeritics AutoPore III 9410), assuming a surface tension and contact angle of mercury of 485 mN/m and 130° , respectively.

3. Results and discussion

3.1. Optimizing the gel-casting process to the temperature range for expansion of the microspheres

The expandable microspheres have been used as a sacrificial template for direct casting of macroporous ceramic bodies. The polymer shell of the microspheres softens with increasing temperature as the glass transition temperature of the thermoplastic co-polymer is reached. Parallel to this process, the liquid hydrocarbon encapsulated inside the gas tight shell will expand and thus increase the internal pressure of the microspheres. These two coupled processes, the softening of the polymer shell and the increase of the internal pressure induce a dramatic volume expansion of more than 40 times when the temperature becomes sufficiently high.³⁷

According to the thermal mechanical analysis (TMA) performed in air by the supplier, the three different microspheres used in this work are expected to start to expand at $76\text{--}81\text{ }^{\circ}\text{C}$ (820DU40), $88\text{ }^{\circ}\text{C}$ (ON316WUX) and $95\text{--}100\text{ }^{\circ}\text{C}$ (551DU40) respectively.³⁷ The difference in the expansion temperature is related to variations in the co-polymer composition and the corresponding glass transition temperature of the thermoplastic shell. It should be noted that the expansion temperature is related to the heating rate and that the TMA data was obtained at a relatively high heating rate of $20\text{ }^{\circ}\text{C min}^{-1}$. We have found that the microspheres expand also at temperatures slightly below the specified on-set temperature at a heating rate of $5\text{ }^{\circ}\text{C min}^{-1}$ and that the chosen process temperature of $80\text{ }^{\circ}\text{C}$ is sufficient to expand the microspheres in suspension if the temperature is held at least 25 min.

It is essential that the setting and consolidation of the concentrated ceramic powder suspension does not occur prior to the

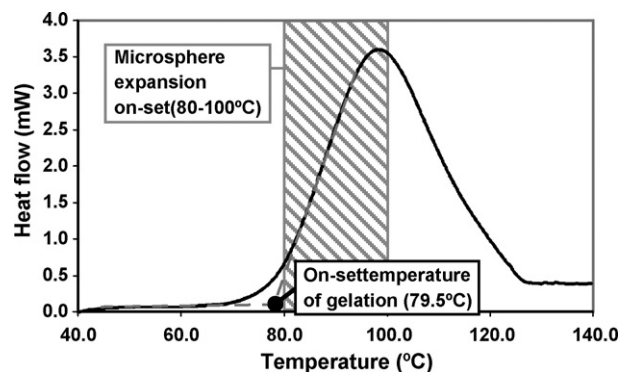


Fig. 2. Differential scanning calorimetry (DSC) measurement (heating rate $5\text{ }^{\circ}\text{C min}^{-1}$) of the alumina gel-casting suspension. The graph displays the heat flow (mW) as a function of temperature ($^{\circ}\text{C}$), where a positive signal is equivalent to an exothermic reaction. The striped area indicates the temperature range for the on-set of microsphere expansion.

maximum expansion of the microspheres to avoid the build-up of internal stresses that can lead to cracking and warping. A low process temperature of $80\text{ }^{\circ}\text{C}$ was chosen to be able to control the microsphere expansion and minimize problems related to water evaporation.

The catalyst was removed and the amount of initiator adjusted to tune the on-set temperature of the gel-casting suspension. Commonly *N,N,N,N'*-tetramethylethylenediamine (TEMED) $(\text{CH}_3)_2\text{NCH}_2\text{CH}_2\text{N}(\text{CH}_3)_2$ is added as a catalyst to the particular monomer cross-linker system (MA–MBAM) used in this study.³⁸ We have chosen not to add any catalyst, which increases the polymerisation temperature of the gel-casting suspension. Fig. 2 shows that by optimizing the amount of initiator (APS) it is possible to achieve an on-set of the gel-casting/polymerisation reaction close to $80\text{ }^{\circ}\text{C}$ (at a heating rate of $5\text{ }^{\circ}\text{C min}^{-1}$). Polymerisation is an exothermic reaction and its on-set temperature is defined as the intersection of the baseline with the extrapolated linear section of the ascending peak slope.

One of the advantages of using expandable spheres as a sacrificial template material is that the total amount of organic material is relatively low, even at final porosities of 80 vol% or above. The thermogravimetric data in Fig. 3 shows that the total

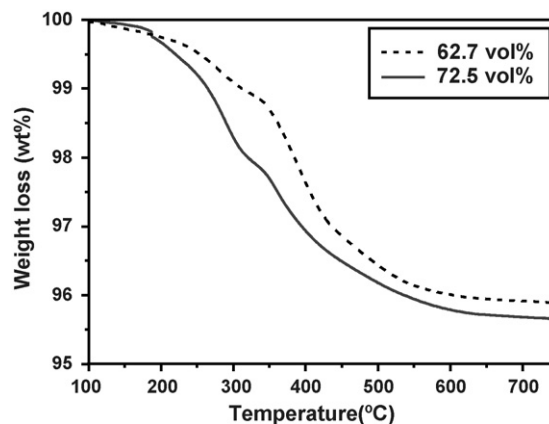


Fig. 3. Thermogravimetric (TG) analysis (heating rate $10\text{ }^{\circ}\text{C min}^{-1}$) in dry air of alumina green bodies at various final porosities (and thus varying initial amounts of expandable microspheres).

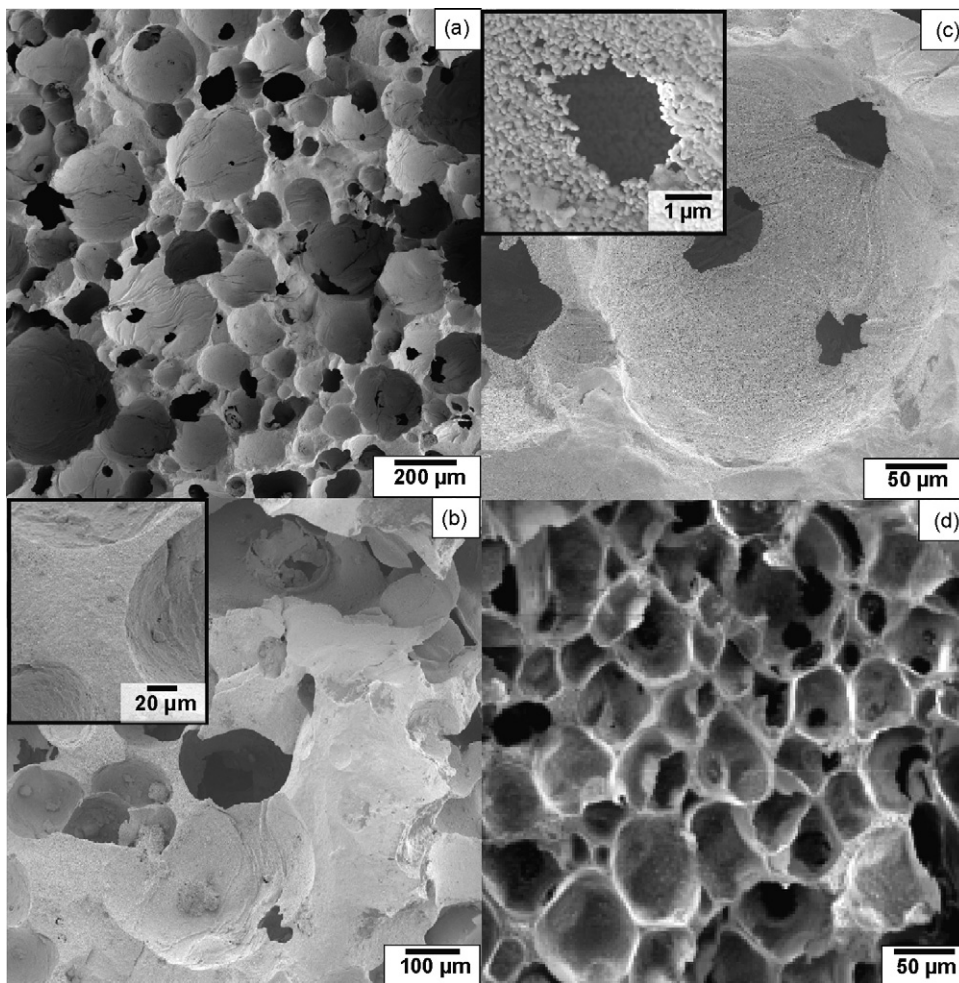


Fig. 4. SEM images of fracture surfaces of macroporous alumina bodies at different porosities. In (a) the porosity is 82.4 vol%. In (b) the porosity is 70.7 vol%. The inset shows a representative image of dense struts separating three pores. (c) Magnification of a pore from a body at 72.6 vol% porosity showing a pore with several cell windows; the inset shows a cell window with a thin wall of single alumina grains. In (d) the porosity is 86.1 vol%.

weight loss is relatively small and remains below 5 wt.% even when a large amount of microspheres is added to reach a final porosity of 72.5 vol%. In fact, it is the polymerised monomers and cross-linker that constitute the major source of the organic additives in the cast bodies amounting to about 4 wt.% with respect to the alumina. It is sufficient to add less than 1–2 wt.% of expandable microspheres even when the final porosity of the material is above 80 vol%.

3.2. Effect of the amount and size of the expandable spheres on the porosity and pore size

Fig. 4 shows typical fracture surfaces of alumina bodies with porosities ranging from 71 to 86%. The expandable microsphere ON316WUX was used to produce the materials in Fig. 4(a–c) while 551DU40 was used in the highly porous material shown in Fig. 4(d). It is clear that the internal pressure in the expanding microspheres is sufficient to result in unconstrained expansion that yields spherical pores after template removal. The pores are homogeneously distributed and the struts are dense. A strut

is a structural component of the cell wall and a dense strut is important for the mechanical stability.²⁷

The cell walls are generally thin in these highly porous alumina bodies; see, e.g. Fig. 4(a). Comparison of Fig. 4(a) and (d) suggests that the use of a smaller microsphere results in smaller pores and that the associated pore walls are thinner compared to the materials with larger pores. Indeed, simple geometric considerations suggest that the (average) wall thickness should be inversely related to the pore size at equal porosities. When the amount of microspheres becomes sufficiently high, it is observed that a significant fraction of the pores are connected; hence the porosity becomes more and more open as the total porosity increases. As the microspheres are squeezed together the alumina grains are forced aside and eventually leave a hole, see, e.g. Fig. 4(c). The contact area between two spheres that are forced together will be spherical or oval, which explains the shape of the cell windows.

Fig. 5 illustrates that the pore size distribution can be controlled by using expandable microspheres of different sizes. The pores originating from the expandable microsphere ON316WUX with an initial diameter (D_{50}) of 33 μm (before expansion), shown

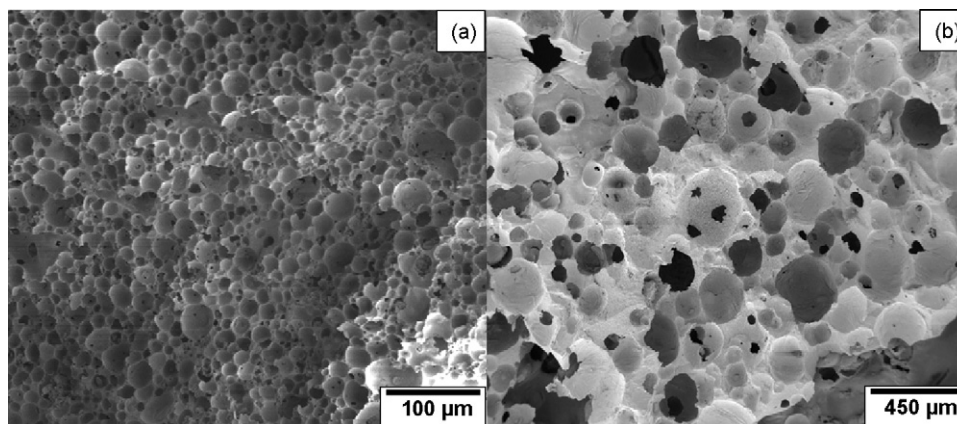


Fig. 5. SEM images of fracture surfaces of porous alumina bodies where microspheres of different sizes were used to create macroporous bodies of similar porosity (in (a) 83.7 vol% and in (b) 82.4 vol%) but different pore size distribution. In (a) the mean microsphere size in the unexpanded state is 10–16 μm . In (b) the mean microsphere size in the unexpanded state is 33 μm .

in Fig. 5(b), are significantly larger than the pores obtained with the expandable sphere 820DU40 with an initial diameter of 10–16 μm .

3.3. Tuning the porosity

Fig. 6 shows that it is possible to tune the porosity and relative density by simply controlling the added amount of the expandable microspheres to the alumina suspension; the porosity clearly scales with the amount of added microspheres (ON316WUX). We find that the mercury porosimetry results in slightly lower porosities compared to the water intrusion measurements. This is not surprising considering that water will wet the alumina and thus enter smaller pores than mercury. The mercury porosimetry measurements which show a bimodal pore size distribution with two major peaks at 0.1 and 100 μm indicate that the porosity in the range around 0.1 μm originates from the interparticle voids in the presintered structure. The closed porosity derived from water intrusion measurements is below 2.5 vol% and is therefore considered negligible.

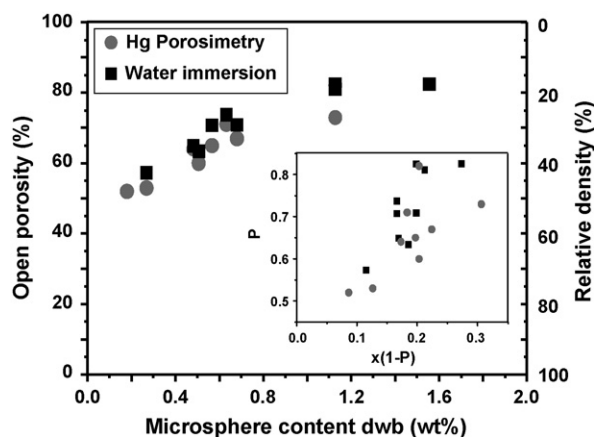


Fig. 6. Open porosity and relative density in presintered porous alumina evaluated by water intrusion and mercury porosimetry as a function of amount of added expandable microspheres. The inset shows the open porosity (P) as a function of $x(1 - P)$ where x is the microsphere content in wt.% dry weight basis (dwb).

Fig. 6 shows that the open porosity increases with the amount of added microspheres following a non-linear relationship. The pore volume generated by the microspheres in the presintered alumina can be expressed as the quotient of the amount of added microspheres in wt.% (x) and the density of the expanded microspheres (y) in g cm^{-3} , assuming a density of 4.0 g cm^{-3} for alumina. The total porosity (P) has two contributions: the porosity generated by the microspheres (x/y), and the porosity originating from the interparticle voids in the presintered alumina (P_0). This can be expressed as

$$P = \frac{x/y + P_0 \times 25/(1 - P_0)}{x/y + P_0 \times 25/(1 - P_0) + 25} \quad (1)$$

which by rearrangement yields:

$$P = \frac{x(1 - P)}{y(P_0 \times 25/(1 - P_0) + 25)} + P_0 \quad (2)$$

The inset in Fig. 6 shows the porosity (P) evaluated with water immersion and Hg porosimetry as a function of added microsphere content (x) multiplied with $(1 - P)$. Although the data display a significant scatter, linear regression of the water immersion data yields a porosity of presintered alumina (without any addition of expandable microspheres) of 41 vol% and a microsphere density after expansion (y) of 0.014 g cm^{-3} .

3.4. Zero external pressure injection moulding: utilizing the internal volume expansion for direct casting of complex-shaped macroporous bodies

The volume expansion of the microspheres provides a possibility to use this novel casting technique to produce near-net shaped macroporous bodies. The process proceeds in a manner very similar to baking; the microsphere expansion induces a volume expansion where the suspension eventually fills the mould and the parallel gelation of the monomer and cross-linker consolidates the expanded suspension. Hence, it is possible to partially fill a mould with the suspension that contains the unexpanded microspheres, close the mould and then heat it to induce the spheres to expand and thus force the suspension to fill the mould.

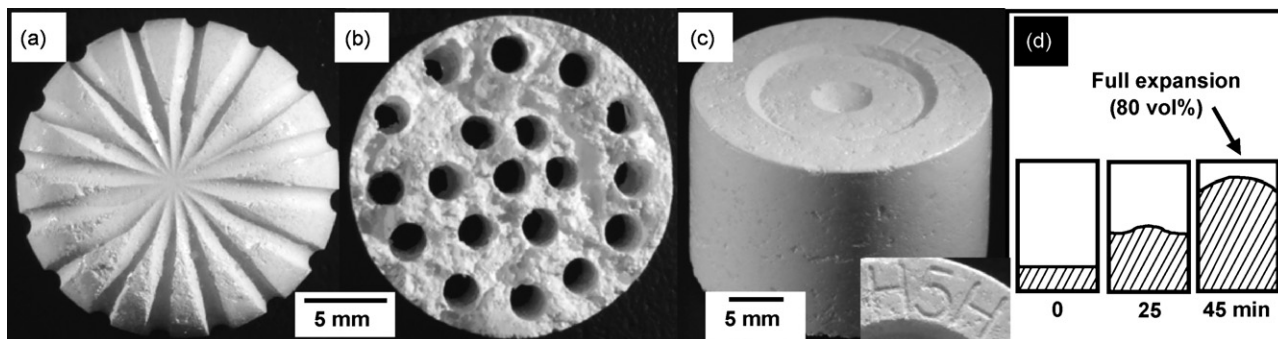


Fig. 7. Macroporous bodies of both cylindrical and complex shape that have been produced by using the gas-filled microspheres as an expandable pore former in the gel-casting suspension. (a) Demonstrates that the surface patterns of an acrylonitrile butadiene styrene (ABS) mould (contact lens container) has been reproduced with great detail. (b) Shows that a pattern of elongated channels are integrated into the macroporous, gel-cast material. (c) Shows a cylindrical body that has been cast in a high-density polyethylene mould with the surface details well reproduced. The schematic picture in (d) shows how the level of a suspension that contains a significant amount of expandable microspheres varies with time; prior to heating (0 min); when the suspension first reaches 80 °C (25 min) and when expansion is complete (45 min).

The suspension then sets when the monomers and cross-linkers polymerise. Fig. 7 illustrates different types of macroporous alumina bodies that can be cast by this novel near-net shape casting technique. The excellent replication of the surface features suggests that the internal pressure that the microsphere expansion induces is sufficient for the suspension to completely fill the mould prior to setting. By inspecting the global pore distribution of the cast bodies we observe that the largest macropores are concentrated to the upper, dome-shaped part of the cast cylinders.

Fig. 7(d) is an attempt to schematically describe how the suspension fills a cylindrical mould as the microspheres expand. The suspension increases in height much like a baking cake generating a dome-shaped top. We have utilized this effect to create a porous monolith with a hierarchical porosity (Fig. 7(b)). A cylinder with several cylindrical rods that are distributed parallel to the surface of the outer cylinder surface and are perpendicular to the circular base and top of the cylinder was filled to one fifth with the pore-forming suspension. Heating the suspension induces a volume expansion around the cylindrical rods. Burning out the organic templating material yields a material with porosity at three different length scales; the cylindrical channels are the largest pores, the intermediate porosity stems from the sacrificial expandable microspheres and there is also a macroporosity with a much smaller pore size distribution that originates from the interstices between the presintered alumina grains.

4. Conclusions

We show that gas-filled microspheres can be used as a sacrificial templating material to produce macroporous ceramic bodies. This novel process utilizes the temperature-induced volume expansion of commercially available microspheres, caused by the softening of the polymer shell and the increase of the internal pressure, to create macropores inside a powder suspension that is consolidated by gel-casting. The on-set of the polymerisation of the gel-casting suspension was designed to match the thermally induced expansion of the gas-filled microspheres to avoid cracking and warping.

It is demonstrated that it is possible to tune and tailor the porosity up to 86% and the pore size distribution from 15 up to 150 μm by controlling the amount and size of the expandable microspheres. The expandable microspheres introduce a relatively low amount of templating material to the powder body, which facilitates a fast and simple debinding process. As low amounts as 1–2 wt.% of the microspheres are required to create a final porosity above 80 vol%.

The volume expansion of the microspheres was also used for direct casting of near-net shaped macroporous bodies of complex shape. The internal pressure that the expanding microspheres create is sufficient to force the suspension to fill a closed mould. The surface features of various types of moulds were replicated with a high degree of fidelity and more complex structures with a hierarchical porosity on three different length scales could also be produced. This novel direct casting method using gas-filled microspheres as an expandable sacrificial template can find potential applications in the production of complex-shaped macroporous ceramics as catalyst supports and as bone scaffolds.

Acknowledgements

The Swedish Research Council (VR) is acknowledged for financial support. We thank Jan Nordin at Expancel AB, Sweden for kindly providing the microspheres and the TMA data and Sadae Watanabe Jonsson for providing alumina powder samples. Kjell Jansson is thanked for assistance with the scanning electron microscopy and advice on differential scanning measurements. Roland Krämer is thanked for help with the sample photography and Julia vom Stein for contribution to the experimental work.

References

1. Saggio-Woyansky, J. and Scott, C. E., Processing of porous ceramics. *Am. Ceram. Soc. Bull.*, 1992, **71**, 1674–1682.
2. Green, D. J. and Colombo, P., Cellular ceramics: intriguing structures, novel properties, and innovative applications. *MRS Bull.*, 2003, **28**, 296–300.

3. Scheffler, M. and Colombo, P., *Cellular Ceramics: Structure, Manufacturing, Properties and Applications*. Wiley-VCH, Weinheim, 2005, 645 pp.
4. Gauckler, L. J., Waeber, M. M., Conti, C. and Jacob-Dulière, M., Industrial application of open ceramic foam for molten metal filtration. *Light Met.*, 1985, 1261–1283.
5. Antsiferov, V. N. and Porozova, S. E., Foam ceramic filters for molten metals: reality and prospects. *Powder Metall. Met. Ceram.*, 2003, **42**, 474–476.
6. Chen, F., Huang, X., Wang, Y., Zhang, Y. and Hu, Z., Investigation on foam ceramic filter to remove inclusions in revert superalloy. *Mater. Lett.*, 1998, **34**, 372–376.
7. Richardson, J. T., Peng, Y. and Remue, D., Properties of ceramic foam catalyst supports: pressure drop. *Appl. Catal. A: Gen.*, 2000, **204**, 19–32.
8. Peng, Y. and Richardson, J. T., Properties of ceramic foam catalyst supports: one-dimensional and two-dimensional heat transfer correlations. *Appl. Catal. A: Gen.*, 2004, **266**, 235–244.
9. Christian, Mitchell, M., Kim, D. and Kenis, P. J. A., Ceramic microreactors for on-site hydrogen production. *J. Catal.*, 2006, **241**, 235–242.
10. Helfferich, R. L. and Schenck, R. C., Kiln furniture for the firing of ceramic articles. European Patent 127808, December 2, 1987.
11. Ramay, H. R. R. and Zhang, M., Biphasic calcium phosphate nanocomposite porous scaffolds for load-bearing bone tissue engineering. *Biomaterials*, 2004, **25**, 5171–5180.
12. Hench, L. L., Bioceramics. *J. Am. Ceram. Soc.*, 1998, **81**, 1705–1728.
13. Hutmacher, D. W., Scaffolds in tissue engineering bone and cartilage. *Biomaterials*, 2000, **21**, 2529–2543.
14. Zampieri, A., Colombo, P., Mabande, G. T. P., Selvam, T., Schwieger, W. and Scheffler, F., Zeolite coatings on microcellular ceramic foams: a novel process route to microreactor and microseparator devices. *Adv. Mater.*, 2004, **16**, 819–823.
15. Montanaro, L., Jorand, Y., Fantozzi, G. and Negro, A., Ceramic foams by powder processing. *J. Eur. Ceram. Soc.*, 1998, **18**, 1339–1350.
16. Taslicukur, Z., Balaban, C. and Kuskonmaz, N., Production of ceramic foam filters for molten metal filtration using expanded polystyrene. *J. Eur. Ceram. Soc.*, 2007, **27**, 637–640.
17. Burg, K. J. L., Porter, S. and Kellam, J. F., Biomaterial developments for bone tissue engineering. *Biomaterials*, 2000, **21**, 2347–2359.
18. Freyman, T. M., Yannas, I. V. and Gibson, L. J., Cellular materials as porous scaffolds for tissue engineering. *Prog. Mater. Sci.*, 2001, **46**, 273–282.
19. Ayers, R. A., Simske, S. J., Nunes, C. R. and Wolford, L. M., Long-term bone ingrowth and residual microhardness of porous block hydroxyapatite implants in humans. *J. Oral Maxillofac. Surg.*, 1998, **56**, 1297–1301.
20. Cerroni, L., Filocamo, R., Fabbri, M., Piconi, C., Caropreso, S. and Condò, S. G., Growth of osteoblast-like cells on porous hydroxyapatite ceramics: an in vitro study. *Biomol. Eng.*, 2002, **19**, 119–124.
21. Ramay, H. R. and Zhang, M., Preparation of porous hydroxyapatite scaffolds by combination of the gel-casting and polymer sponge methods. *Biomaterials*, 2003, **24**, 3293–3302.
22. Bose, S., Darsell, J., Hosick, H. L., Yang, L., Sarkar, D. K. and Bandyopadhyay, A. E., Processing and characterization of porous alumina scaffolds. *J. Mater. Sci. Mater. Med.*, 2002, **13**, 23–28.
23. Studart, A. R., Gonzenbach, U. T., Tervoort, E. and Gauckler, L. J., Processing routes to macroporous ceramics: a review. *J. Am. Ceram. Soc.*, 2006, **89**, 1771–1789.
24. Galassi, C., Processing of porous ceramics: piezoelectric materials. *J. Eur. Ceram. Soc.*, 2006, **26**, 2951–2958.
25. Colombo, P., Conventional and novel processing methods for cellular ceramics. *Phil. Trans. R. Soc. A*, 2006, **364**, 109–124.
26. Sepulveda, P., Gelcasting foams for porous ceramics. *Am. Ceram. Soc. Bull.*, 1997, **76**, 61–65.
27. Gibson, L. J. and Ashby, M. F., *Cellular Solids: Structure and Properties*. Cambridge University Press, Cambridge, 1997, 510 pp.
28. Tang, F., Fudouzi, H., Uchikoshi, T. and Sakka, Y., Preparation of porous materials with controlled pore size and porosity. *J. Eur. Ceram. Soc.*, 2004, **24**, 341–344.
29. Colombo, P. and Bernardo, E., Macro- and micro-cellular porous ceramics from preceramic polymers. *Composites Sci. Technol.*, 2003, **63**, 2353–2359.
30. Pickrell, G. R., Butcher, K. R. and Lin, C. L., Porous articles and method for the manufacture thereof. European Patent 10/444714, August 10, 2004.
31. Kim, Y., Jin, Y., Chun, Y., Song, I. and Kim, H., A simple pressing route to closed-cell microcellular ceramics. *Scripta Mater.*, 2005, **53**, 921–925.
32. Lyckfeldt, O. and Ferreira, J. M. F., Processing of porous ceramics by ‘starch consolidation’. *J. Eur. Ceram. Soc.*, 1998, **18**, 131–140.
33. Ortega, F. S., Sepulveda, P., Innocentini, M. D. M. and Pandolfelli, V. C., Surfactants: a necessity for producing porous ceramics. *Am. Ceram. Soc. Bull.*, 2001, **80**, 37–42.
34. Du, Z., Bilbao-Montoya, M. P., Binks, B. P., Dickinson, E., Ettelaie, R. and Murray, B. S., Outstanding stability of particle-stabilized bubbles. *Langmuir*, 2003, **19**, 3106–3108.
35. Tomalino, M. and Bianchini, G., Heat-expandable microspheres for car protection production. *Prog. Org. Coat.*, 1997, **32**, 17–24.
36. Griss, P., Andersson, H. and Stemme, G., Expandable microspheres for the handling of liquids. *Lab Chip*, 2002, **2**, 117–120.
37. Private communication Jan Nordin, Expancel, Sweden.
38. Potoczek, M. and Zawadzak, E., Initiator effect on the gelcasting properties of alumina in a system involving low-toxic monomers. *Ceram. Int.*, 2004, **30**, 793–799.